

Received: 26 January 2022 • Accepted: 09 March 2022

## Research

doi: 10.22034/jcema.2022.326658.1076

# Investigating Shear Bands Propagation in Sands by Using the Developed Elemental-like Direct Shear-faulting Box

Ahmad Khaleghi \*, Mojtaba Moosavi, Mohammadkazem Jafari

International Institute of Earthquake Engineering and Seismology, Tehran, Iran.

\*Correspondence should be addressed to Ahmad Khaleghi, International Institute of Earthquake Engineering and Seismology, Tehran, Iran. Tel: +98 937 585 2644; Email: [ahmadkhaleghi1992@yahoo.com](mailto:ahmadkhaleghi1992@yahoo.com)

## ABSTRACT

This study investigates faults propagation in granular soils using the developed elemental-like direct shear-faulting box by detecting shear bands formation within soil samples. For this sake, first, some modifications are applied to the direct shear box in the Earthquake Research Institute. In this regard, two blocks are built at an angle of 45 degrees that can be moved relative to each other. Transparent walls are employed to increase the static resistance. Moreover, four screws are installed on the floor of the device. The friction in the test is reduced by using several ball bearings. The required thickness for the box walls is determined using a numerical simulation in ABAQUS software. To investigate faulting in granular soils, Firoozkooh sand is utilized and placed in the developed shear box. The overhead load is modeled by applying air pressure to a rubber membrane containing water. By continuous imaging of soil profiles, alterations in the soil surface are recorded, and an image correlation method is employed to predict the amount of fault-induced displacements, strains, and dilations. Results verify that the dilation effect elevates with increasing moisture content and wanes with the addition of fine-grained percentage and by boosting vertical loads. Moreover, various behavior has been observed without softening for cementitious sands.

**Keywords:** Faults propagation Developed elemental-like direct shear-faulting box, Firoozkooh sand, Digital image correlation method

Copyright © 2022 Ahmad Khaleghi. This is an open access paper distributed under the [Creative Commons Attribution License](#). *Journal of Civil Engineering and Materials Application* is published by [Pendar Pub](#); Journal p-ISSN 2676-332X; Journal e-ISSN 2588-2880.

## 1. INTRODUCTION

Available studies acknowledge that due to the movement of bedrocks and faults, rupture spreads to the earth's surface, which is usually accompanied by relative displacements. In most cases, these relative displacements create irreversible damage to the structures. Two earthquakes in Turkey [1], [2], and Taiwan [3] indicated that shallow faults have deleterious effects on structural buildings and infrastructures. To alleviate these effects, one should avoid constructing in the danger zone. It needs to determine the location of a potential earthquake-induced by a surface fault rupture. To analyze faults rupture propagation, the localization of shear deformations known as shear bands should be studied [4]. The localization of shear strain theory is

developed by Tomas for non-elastic porous media [5]. This theory has been utilized to forecast shear bands propagation [6]. Investigating shear bands still has various unknown aspects; nevertheless, it can lead to a more accurate prediction of surface faulting [7]. Owing to the inherent heterogeneity of soil materials and varieties in the type of sands, different reports have been mentioned in the technical literature, claiming that a comprehensive model for estimating the shear bands in all sandy soils has not yet been developed. Investigating the key factors related to shear bands propagation can contribute to a better understanding of the constitutive models of sandy soil. By assessing the existing faults and the amount of safety provided in the structures, it is plausible to estimate the

possible damages caused by an earthquake. Earthquake deformations are made up of two separate parts. Part of it is devoted to the vibrations during an earthquake. The second part is, in fact, the permanent displacements that occur due to a fault rupture propagation [8]. The phenomenon of faulting is practically a kind of shear localization and shear bands formation [9]. Therefore, evaluating the shear bands in the soil not only leads to a better prediction of fault propagation but also provides an approach to reducing potential damages. Assessing shear bands formation in granular soils started in the 80s at the University of Cambridge in many types of research and then during the 2000s onwards due to the critical significance of structures and the formation of faults on the surface [10]. Various numerical models on shear band formation have been proposed in the literature so far [10], [11], [12]; nevertheless, the employed simplification assumptions may mitigate the ability of numerical models to accurately predict fault rupture propagation, and thus, physical models need to be provided. In a study, Joer et al. [13] presented a report on the construction and operation of a shear box to study the behavior of granular materials such as sandy soils. The device relies on its kinematic control, which allows the simulation of plane strain conditions for the sample. The purpose of making this device is to study the deformation of granular materials under the conditions of rotation of the main stress and strain planes. In this report, they first examined the various design options of the device and then investigated the results of isotropic experiments in fixed volume conditions with and without rotation of the main stress and strain planes. Their results showed that the reciprocating property of the rotation of the main planes generates liquefaction in the soil. Lo et al. [14] developed a new multiaxial cell for strain-softening experiments. One of the advantages of this device is its ability to create large strains in the sample without causing defects in boundary conditions, which allows the formation of shear bands and strain path control. In their research, they presented the results of strain softening under multiaxial stress in quartz sandy soil using the fabricated device. Both stress and strain path tests were performed. In the stress path test, the sample was loaded along the main axis in the control deformation mode, and the stress response along a predetermined path was limited to a certain value using a computer that allows the strain-softening to be observed in a controlled manner. Two types of softness were identified, including pre-rupture and post-rupture. In the

case in which softening occurs before the rupture, the generated deformation was homogeneous. In the post-rupture mode, a slight deformation occurred homogeneously, and eventually, a shear band was formed. Stone and Brown [15] proposed a new system for simulating ground subsidence in centrifuge models. The most important application of this system is to predict subsidence in mines. In their study, a brief review of extraction methods was performed, and the performance of the proposed system in generalizing these methods was indicated in centrifuge model experiments. In addition, the ability of the system to determine land loss or boundary deformation issues was examined. If a comparison is made between wet soils, the lowest shear zone is related to wet soils with 5% moisture. If the percentage of moisture increases, the shear zone would also increase. However, in all cases, the dimensions of the shear zone are smaller in comparison with dry tests. Due to the apparent adhesion in wet soils, the soil does not allow the development of shear bands on a large surface. In other words, if the soil is not cohesive, by creating a shear displacement in the sample, each grain easily affects its adjacent grain. Whereas, due to the presence of water bridges between the sand grains and apparent adhesion, the fault energy is used to break the band between the grains. Therefore, less area is distorted. In previous studies, various devices were made to perform direct shear experiments on soil samples. ASTM-1990-Vol 13- p48 [16] proposed a box. The device is capable of applying horizontal displacement in three stages of 7.6 mm. This device can perform tensile testing in one direction. It also has transparent walls on both sides and is suitable for airbag usage. ASTM-1992-Vol15-p129 [16] produced a device called 1γ2ε. This device can be changed in the horizontal dimension between 550 to 687 mm, which corresponds to a strain of 22%. Also, In the vertical dimension, it can change from 413 to 550 mm, corresponding to a strain of 28%. Moreover, Volumetric strain can increase up to 20%. This device is also transparent on both faces. ASTM-1994-Vol17-p125 invented a device that can perform the direct shear test in two horizontal directions and has dimensions of [16]. In this research, by evolving the facilities available in the Earthquake Research Institute in Tehran, Iran, an attempt has been made to study shear bands formation. To better understand the behavior of sandy soils, some key factors such as density, soil grain size, average and maximum grain size as well as effective stress levels were assessed with the aid of the image processing technique.

## 2. METHODOLOGY

### 2.1. CONSTRUCTION OF THE DEVELOPED (ELEMENTAL-LIKE) SHEAR\_FAULTING BOX

Faults are known as fractures with relative displacements, where displacements are parallel to the fault's surface. Based on the direction of the surface in which faults occur, they are divided into two separate categories. Faults are

generated from horizontal slippage, and faults are induced by vertical slippage. To investigate faults behavior, a physical model has been developed in this study by evolving the typical direct shear box available in the

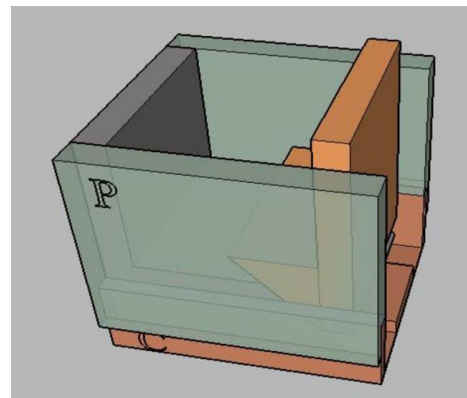
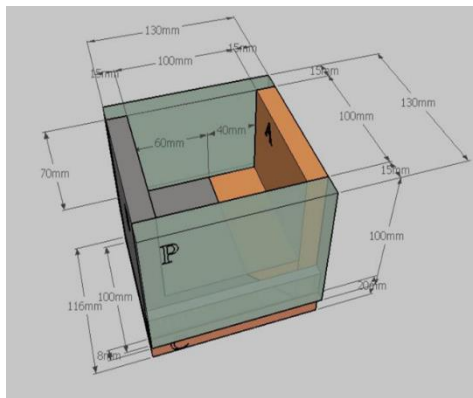
Earthquake Research Institute. The direct shear box is modified by altering some details in the use of clamps, ball bearings (Figure 1) on the fault wall, and screws.



**Figure 1.** Ball bearings used in this study

Embedding ball bearings leads to the reduction of friction forces and results in more accurate results. The advanced 1-g elemental-like shear box can practically reverse model faults at the angle of 45°. To determine an optimal value for the walls' thickness, a simple simulation study has been carried out in ABAQUS software. To precisely utilize the box, the soil is considered at the height of 4 cm from the floor. Thus, the height of the developed box is considered to be 4 cm longer than a typical box. Figure 2 displays the schematic

configuration of the developed elemental-like shear box. The horizontal force is applied to the box at the rate of 2mm per minute. The studied angle is considered 45 degrees to be comparable to available studies in the literature. The required thickness is determined 15 mm based on a numerical simulation in the ABAQUS software. To increase the resistance of the table of the direct shear box, 4 screws with a length of 3.5 cm are considered in the simulation.



**Figure 2.** Schematic configuration of the developed elemental-like shear box

## 2.2. THE SOIL USED IN THIS STUDY

In this study, Firoozkooh sand is chosen for the analysis. The selected subangular sand has a golden yellow color and a uniform grain size distribution. Based on Laboratory observations (electron microscopy), this sand has 15% full

sharpness, 45% medium sharpness, 10 to 15% complete roundness, and 25 to 30% medium roundness. The physical parameters of the soil (Firoozkooh sand) utilized in this study are mentioned in Table 1.

**Table 1.** Soil parameters considered in this study

Soil type	$G_s$	$e_{max}$	$e_{min}$	$\Delta e$
161	2.65	0.943	0.603	0.34

By assuming relative density of 50 percent (similar to previous studies on this sand), soil porosity is obtained as

$$D_r = \frac{e_{max} - e}{e_{max} - e_{min}} \times 100 \rightarrow 50 = \frac{0.943 - e}{0.943 - 0.603} \times 100 \rightarrow e = 0.77 \quad (1)$$

The obtained porosity is utilized to make the sample. To make a unified sample, the required quantity of sand for a 2.5 cm layer should be predicted.

$$\gamma_d = \frac{2.658 \times 9.81}{1 + 0.77} = 14.73 \text{ kN/m}^3 \quad (2)$$

$$W_d = 2.5 \times a \times b \times \gamma_d = 2.5 \times 10 \times 10 \times 10^{-6} \times \frac{14.73}{9.81} = 375.4 \text{ g} \quad (3)$$

According to Eq. 3, to make a 2.5 cm sample, 375.5 g of Firoozkooh sand is required. The soil sample is embedded inside the box using the sand pluviation technique. For a 2.5 cm soil layer, by assuming the addition of 5% moisture content, about 18.77 g of water is required. After completely mixing the soil with water, the soil is poured

into the test box based on the pluviation technique. The soil is compacted by releasing a metal hammer from a constant height (5 cm). This method yields the porosity and relative density computed above. Note, ZMK2 clay and Portland cement are used to make fine-grained samples and cement samples, respectively.

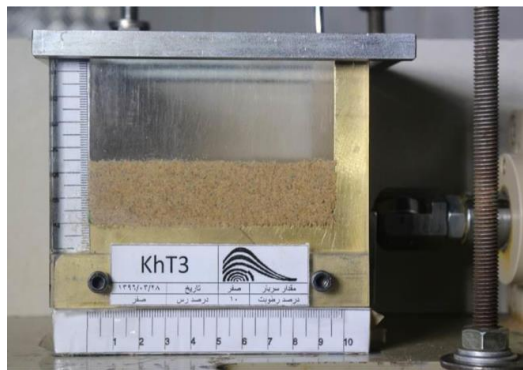
### 2.3. TESTS PROCEDURES

Two types of tests are conducted in this study:

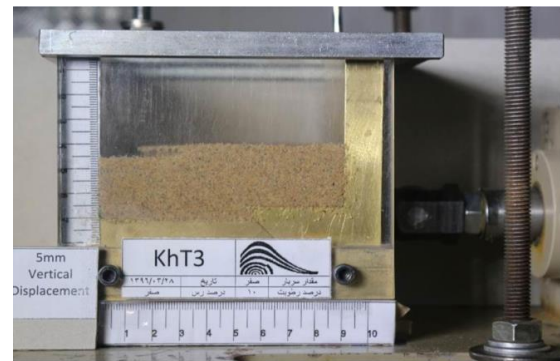
#### I. Tests without surcharge stress

After placing the soil sample, vertical and horizontal stresses are applied to the sample. A horizontal displacement with a speed of 2 mm per minute is applied to the half of the box. By considering this strain, the test approaches quasi-static tests. For every ten degrees of displacement in the vertical gauge equal to 0.1 mm, a

photo is taken, and the ring gauge is read and memorized. It is continuous till the vertical displacements reach 5 mm. The test process takes 150 seconds, and 50 raw images are taken. [Figure 3](#) indicates the soil sample before loading and after the rupture. Fault propagation is obviously visible in [Figure 3b](#).



(a)



(b)

**Figure 3.** Soil sample. (a) before loading, (b) after rupture

#### II. Tests with surcharge stress:

A two-phase plastic cushion (rubber membrane) containing 220 cc of water is utilized to apply the surcharge stress. Then, the required pressure is applied to the cushion through the available air pumps. Since fluid

pressure in all directions is identical, for the air pressure to be applied only to the soil, a rigid device is installed in the body of the box. [Figure 4](#) illustrates the loading cushion on the soil surface.



**Figure 4.** Loading on soil sample using the rubber membrane

To control pore pressure during the tests, a regulator made by Fairchild Company is utilized. This device by

controlling the internal and external fluxes, fixes the pressure-induced within the sample. A non-metric

Canon EOS 350D digital camera is employed with a wireless remote control to take photos of faults. [Table 2](#)

shows the tests conducted by the elemental-like shear-fault box developed in this study.

**Table 2.** the tests conducted by the elemental-like shear-fault box

Row	Number	Water content	Clay percentage	Cement percentage	Surcharge (kPa)
1	KhT1	5	0	0	0
2	KhT2	0	0	0	0
3	KhT3	10	0	0	0
4	KhT4	15	0	0	0
5	KhT5	10	0	0	10
6	KhT6	10	0	0	25
7	KhT7	10	0	0	40
8	KhTV1	15	0	0	0
9	KhTV2	10	0	0	0
10	KhT53	5	0	4	0
11	KhT54	5	0	4	10
12	KhT33	5	5	0	0
13	KhT34	5	5	0	10
14	KhT35	5	5	0	20
15	KhT36	5	5	0	30
16	KhT37	5	10	0	0
17	KhT38	5	10	0	10
18	KhT39	5	10	0	20
19	KhT40	5	10	0	30
20	KhT55	5	0	4	20
21	KhT56	5	0	4	30
22	KhT29	5	15	0	0
23	KhT32	5	15	0	30
24	KhT31	5	15	0	20
25	KhT30	5	15	0	10
26	KhT56	5	0	4	0
27	KhT11	15	0	0	10
28	KhT12	15	0	0	20
29	KhT13	15	0	0	30
30	KhT8	5	0	0	10
31	KhT9	5	0	0	20
32	KhT10	5	0	0	30
33	KhT14	10	0	0	10
34	KhT15	10	0	0	20
35	KhT16	10	0	0	30
36	KhT17	0	0	0	10
37	KhT18	0	0	0	20
38	KhT19	0	0	0	30
39	KhT51	0	5	4	0



## 2.4. DEVELOPMENT OF IMAGE PROCESSING WITH DIGITAL IMAGE CORRELATION METHOD (DIC)

By comparing the photos after and before the soil deflection and using numerical calculations, DIC method predicts soil strains. The mean square error method (MSE)

can be used to obtain the difference between target and temporary pictures.

$$MSE = \frac{\sum \sum \text{Temporary}(x,y) - \text{Target}(x,y)}{\text{Number of pixels}} \quad (4)$$

Where, Temporary ( $x,y$ ), and Target ( $x,y$ ) are the intensity of temporary and target pictures at ( $x,y$ ), respectively.

In the DIC method, the camera should be positioned so that it can take a photo of the two-dimensional surface of the sample in various positions during loading. Since the photos taken are two-dimensional pictures of the sample surface, the estimation of the motion of each point multiplied by the magnification of the imaging system will not be exactly equal to the actual physical point on the sample surface, unless the following requirements are met.

- 1) The surface of the sample should be smooth and remain parallel to the camera sensor during loading. The non-plane motion of the sample should be small enough to be ignored. Non-plane movement of the sample leads to a variation in the magnification of the photographs taken. Thus, the displacement of the page is not accurately evaluated. Naturally, non-plane motion can be reduced to some extent by moving the camera away from the specimen.
- 2) The shooting system should not be geometrically distorted. In an optical imaging system, there is a more or less geometric distortion, which disrupts the ideal linear relationship between the physical point and the image point, which produces additional displacements. If the effects of geometric distortion cannot be ignored, they must be eliminated by employing distortion correction methods so that the measurements are accurate.

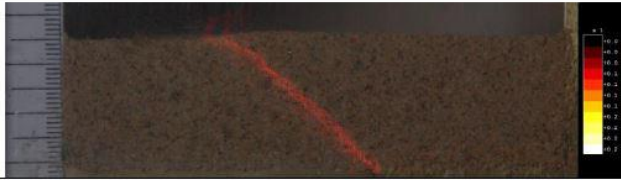





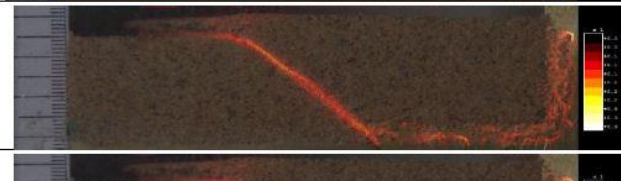

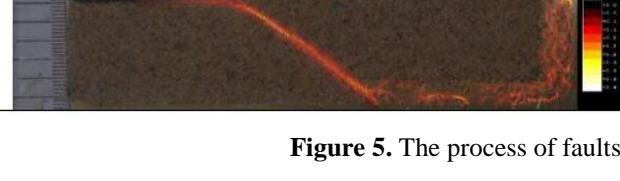
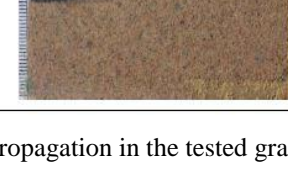
## 3. RESULTS AND DISCUSSION

In this section, part of the results of the experiments performed by using the elemental-like shear-fault box is provided. The most significant characteristics of faults propagation in granular soils are assessed by examining the various experiments performed. [Figure 5](#) indicates the propagation of reverse faults in sandy soil with 5%

Due to the discrete nature of digital photos, accurate displacements with pixel accuracy can be easily calculated. To further improve the accuracy of displacement measurements, special sub-pixel recording algorithms should be utilized. Generally, to achieve sub-pixel accuracy, the execution of two-dimensional DIC involves two consecutive steps. The first step is to evaluate the initial deformation, and the second step is to measure the sub-pixel displacement. That is to say, the two-dimensional DIC method typically requires an accurate initial guess of the deformation before achieving the sub-pixel accuracy. For example, a cross-correlation algorithm (such as the Newton-Raphson method) converges only when an accurate initial conjecture is given.

Usually, the relative deformation or rotation between the reference set and the deformed set is very small. Therefore, it is easy to achieve an accurate assessment of the initial displacements by a simple search method. The exact positions of the deformed set can be determined by a sufficient, pixel-by-pixel, routine search, which is performed within a certain range in the deformed image. The techniques mentioned in most cases are practical. In special cases, problems occur when a large rotation or large deformation occurs between the target set and the temporary set. In this case, some pixels of the target set come out of the hypothetical set in the deformed image. As a result, the similarity between the target set and the hypothetical deformed set is significantly reduced. The method explained above is utilized in this study to investigate faults propagation.

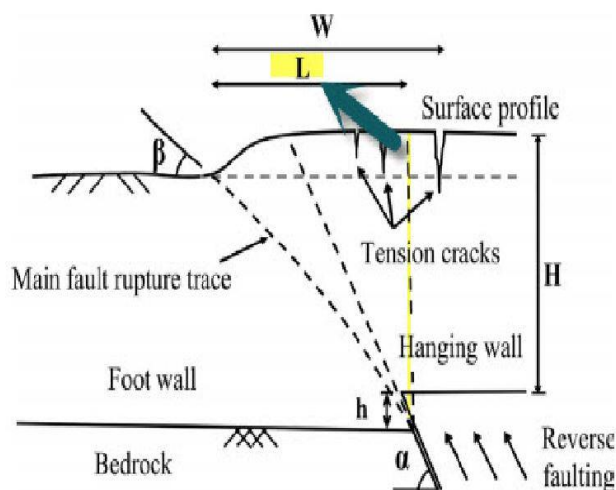
moisture content. It is observed that in small displacements, shear bands are formed on the soil surface. With increasing horizontal displacement by the elemental-like, shear-fault box, the created shear strain increases and appears as a clear outcrop.

output image of the shear bond	raw image of the test	Displacement (mm)	Row
		1	1
		2	2
		3	3
		4	4
		5	5

**Figure 5.** The process of faults propagation in the tested granular soil

The following section discusses different aspects of fault propagation in granular soil. In this regard, the shear bands created in the sample, the amount of fault displacement required for reaching the ground, and the location of the outcrop are examined. Since the mentioned characteristics depend to a large extent on the geo-mechanical properties of the soil, by performing experiments utilizing the elemental-like shear-fault box, the tested soil was evaluated in terms of its strength and deformation. It

should be noted that in this section, the values of  $L$ ,  $h$ ,  $H$ , and other parameters are used according to [Figure 6](#). To observe faults in the soil surface, it is necessary that the horizontal soil displacement be more than a certain amount. In general, in small displacements, part of the displacement is absorbed due to the softening behavior of the soil. If the displacement reaches a certain level, the shear band reaches the initial level, and an outcrop appears.



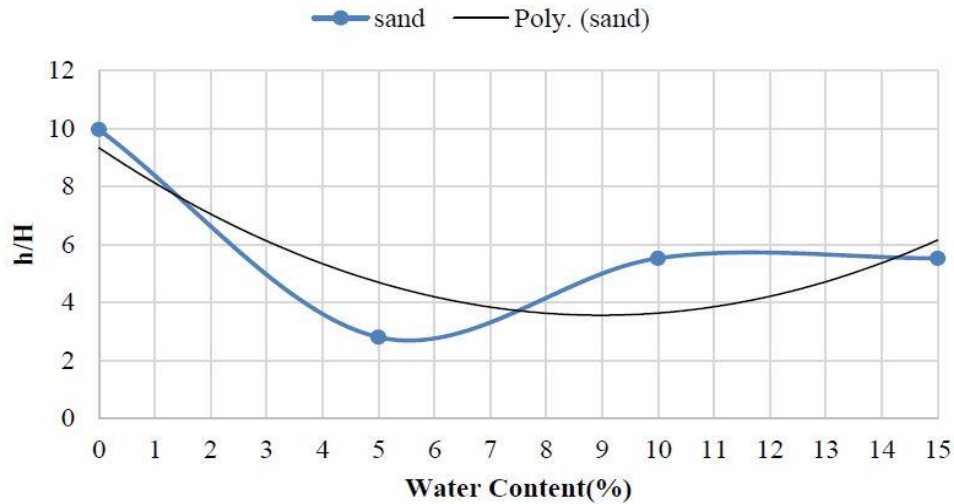
**Figure 6.** Schematic configuration of the model used in this study

[Figure 7](#) shows the changes in the  $h/H$  ratio (percentage) per various water contents. Generally, the value of ( $h$ ) is

normalized to the total soil height and is reported as a percentage of  $h/H$ . The less the value of this ratio, the less

the amount of displacement required for the fault at the soil surface to appear. In statistical analysis, the probability of fault occurrence in the bedrock and in the depths of the earth is estimated, and if the probability of surpassing the amount of  $h/H$  number is small, it can be claimed that the fault has no effect on terrestrial structures. In general, as soil moisture increases, the amount of displacement required for the propagation of faults in the soil surface

decreases, and the lowest rate occurred for 5% humidity. Additionally, [Figure 7](#) shows the ultimate strain changes with respect to moisture. As expected, as the soil moisture increases, the amount of ultimate strain generally decreases. In other words, the more soil moisture percentage, the more brittle behavior it shows.

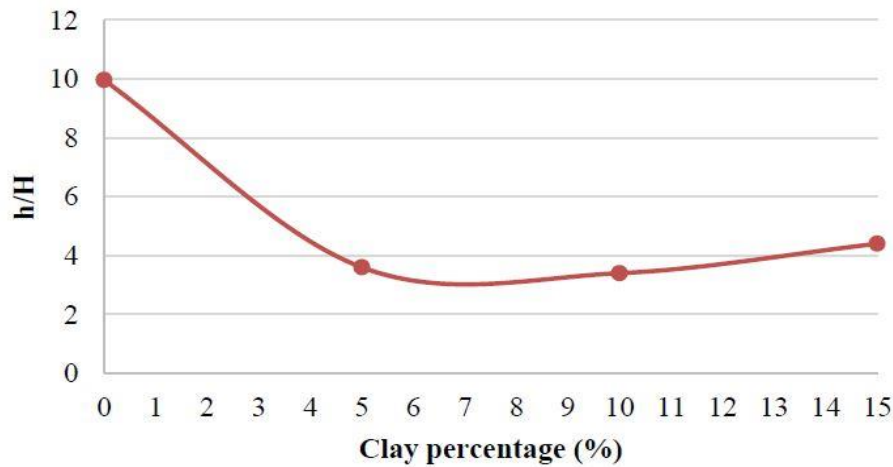


**Figure 7.** The displacement changes required for the fault to reach the surface in different Moisture contents

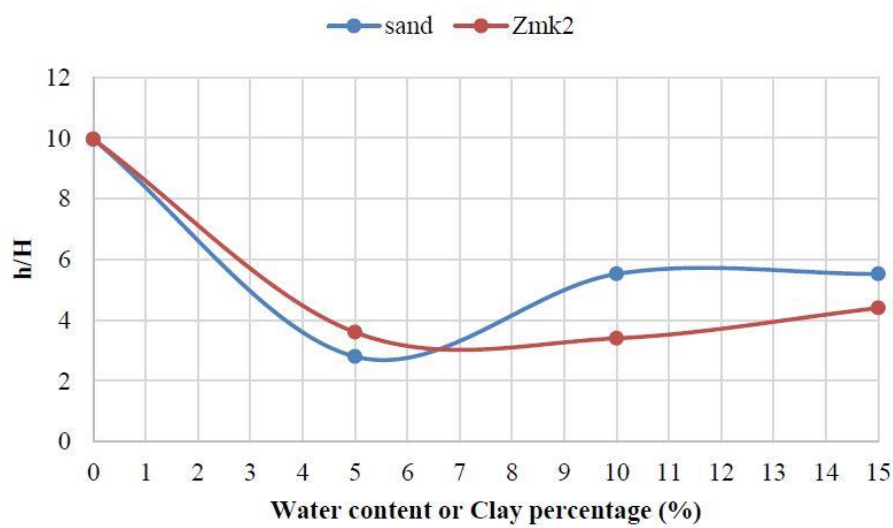
Two important points can be derived from [Figure 7](#). The first point is that there is a significant difference in the amount of  $h/H$  between dry soils and wet soils. The amount of  $h/H$  for dry sandy soils is much higher than its value for wet soils. In fact, in order for the fault to reach the ground, more displacement is required in the bedrock floor. This amount is reduced to about half, on average, in wet sandy soils. In fact, the fault propagation rate in wet soils is much higher than in dry soils. As mentioned earlier, the velocity of the fault displacement, or slip velocity, is directly related to the shear wave velocity. In soils where the shear wave velocity is higher, the value of this parameter will be higher. Therefore, it can be concluded that the shear wave velocity in wet sandy soils is much higher than dry soils. On the other hand, the higher the shear wave velocity, the more brittle the material can be. Therefore, it can be understood that wet soils behave more brittle than dry soils. The same results are observed by Ahmadi et al. [17]. The second point is that by examining the value of  $h/H$  for wet soils, it can be perceived that while these values are very close to each other, a slight difference can be found among them. It seems that sandy soil with 5% moisture content has the lowest value of  $h/H$  and with increasing moisture content, its value also increases slightly. In fact, it can be stated that at about 5% moisture content, wet sandy soil has its most brittle behavior. Understanding this is also better achieved by performing shear-fault

experimental tests. To identify soil behavior, several series of elemental fault-like shear tests were planned. As mentioned before, the reason for choosing the elemental-like shear test was the relatively good proximity of this experiment with the fault propagation phenomenon in a physical modeling. The study of soil behavior at different humidity and under different vertical stresses shows interesting results related to the effect of moisture on soil behavior. Furthermore, as mentioned before, due to the friction of the wall with the soil (even if it is small), the calculation of the fault reaching the ground, from the images of the transparent part of the reservoir, is erroneous and not reliable. Therefore, the measurements were carried out using a caliper with an accuracy of one hundredth of a millimeter. [Figure 8](#) illustrates the variation of  $h/H$  by altering the percentage of kaolinite clay. It seems that the soil with 5% clay is not much affected by its plastic properties. However, by increasing the amount of clay to more than 10 percent, the behavior of mixed and cohesive soil changes drastically and the amount of  $h/H$  tends to a stable value. By comparing the effects of wetting and adding fine-grained particles ([Figures 7 and 8](#)) it can be concluded that wet soil shows more brittle behavior, while cohesive clayey soil has a more flexible behavior. [Figure 9](#) compare the impacts of clay percentage and moisture content on rupture depth. The same behavior is indicated by Ahmadi et al. [17].





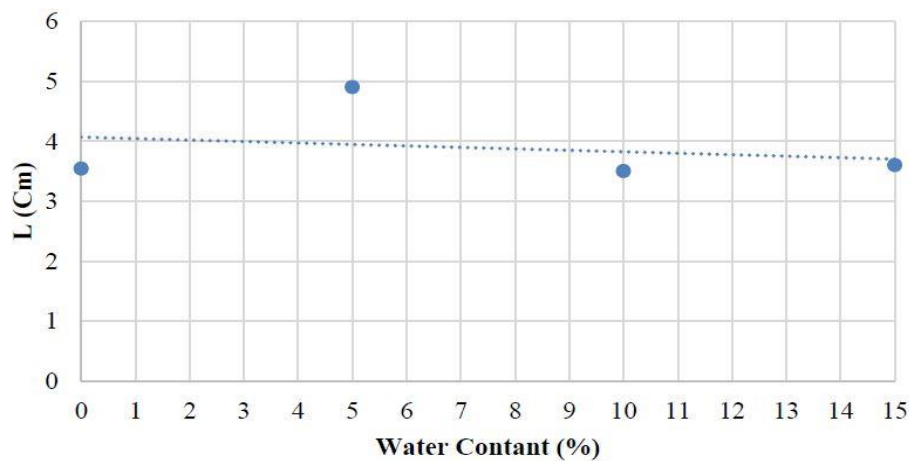
**Figure 8.** Effect of clay percentage on rupture depth



**Figure 9.** Influence of clay percentage and moisture percentage parameters on rupture depth

One of the most important questions to be answered is where the fault appears on the earth's surface after developing within the soil layer. In fact, faults in the bedrock may be partially detected. But the point is, if a fault occurs and develops within the soil, where does the rupture occur on the ground surface? Different parameters can affect the location of fault outcrops. One of the most

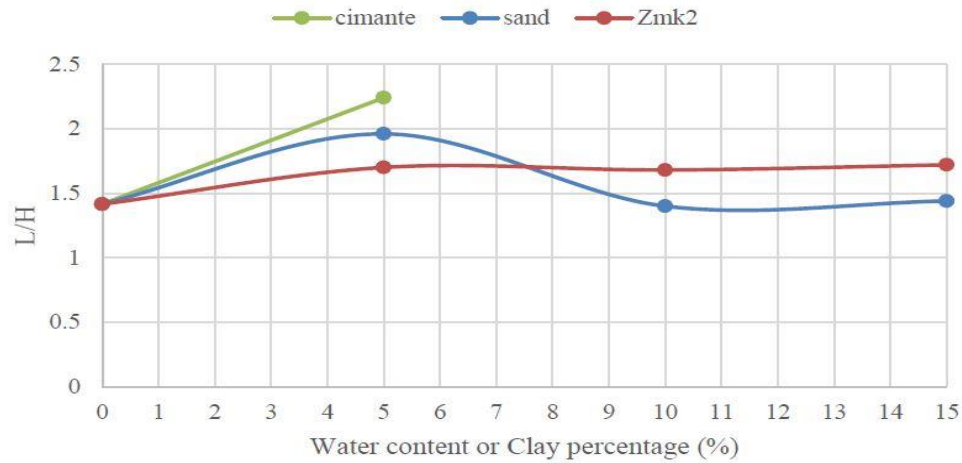
significant of these parameters is the type of fault that has occurred. Generally, the outcrop of normal faults, related to the vertical image of the fault tip in the bedrock, has a shorter distance compared to the reverse fault (parameter L). This comparison is shown in [Figure 10](#). [Figure 10](#) is also in good agreement with the results of Ahmadi et al. [\[17\]](#)



**Figure 10.** Changes in parameter L with soil moisture content in wet fault testing

For each experiment, different shear bands were activated and deactivated during the occurrence of the fault phenomenon. This causes the location of the outcrop on the ground to change at different stages of the fault propagation. [Figure 11](#) displays the changes in the L/H, which somehow represents the fault outcrop at the end of the experiment, with a change in the soil moisture content or clay percentage for different samples. It is observed that after 5% water content, as the moisture content increases,

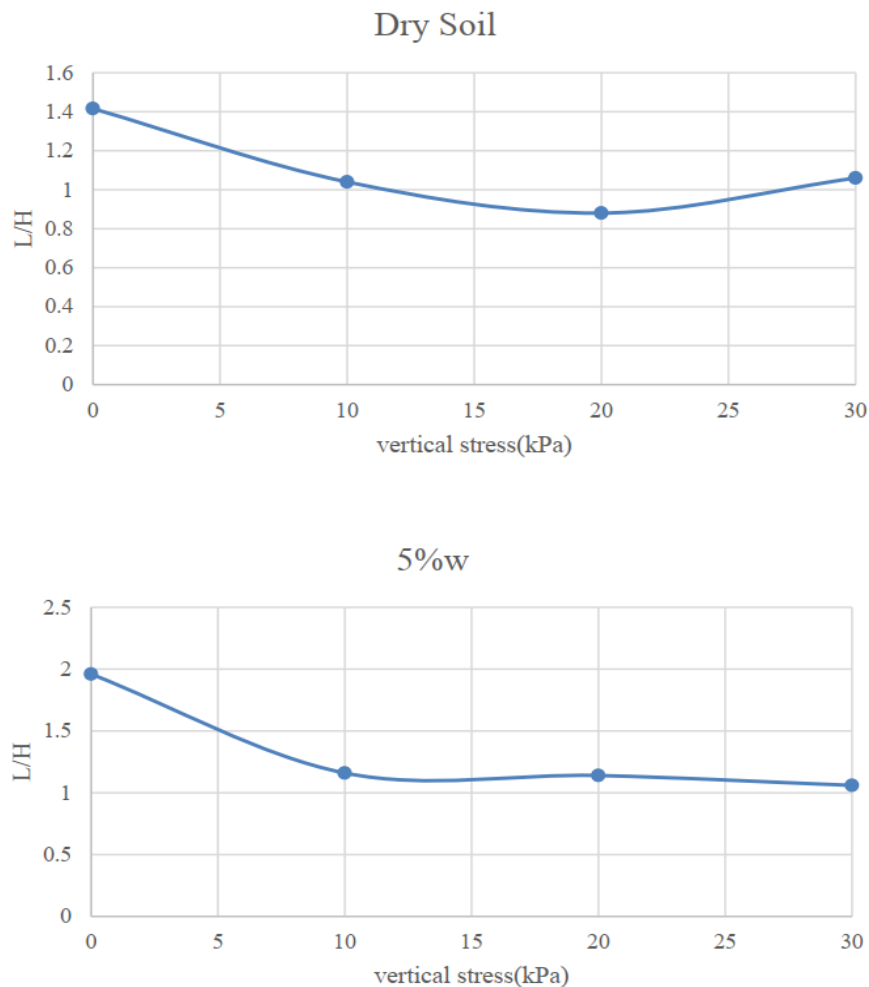
L/H for the sand sample decreases, while other specimens (cemented and Zmk2) indicate different behavior. Reducing this parameter leads to the reduction of the distance between the fault outcrop and the vertical image of the fault tip in the bedrock. It is noteworthy that the output values of the elemental-like device are in good agreement with the experiments available in the literature [\[17\]](#).

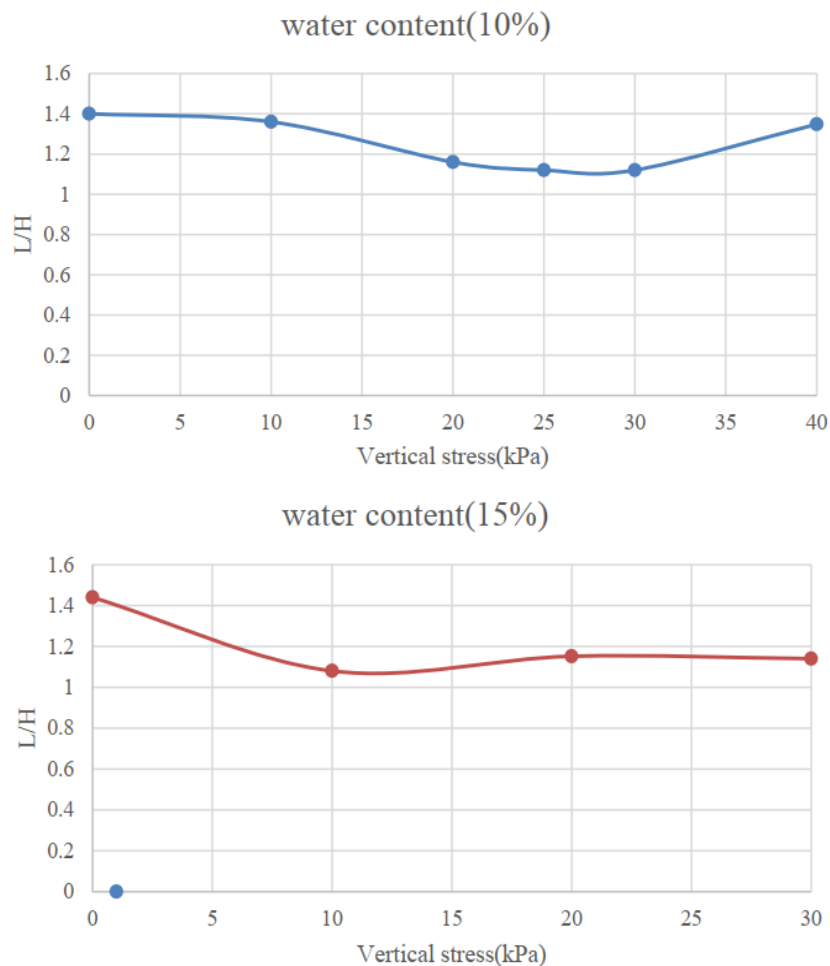


**Figure 11.** changes in L / H parameter with respect to moisture content

The variation of L / H with surcharge shows different behavior in different water contents [\(Figure 12\)](#). A similar

trend is observed for samples with 5% and 15% water contents.





**Figure 12.** Changes in  $L / H$  with overhead variation for different water contents

#### 4. CONCLUSION

In this study, faults propagation in granular soils using the developed elemental-like direct shear-faulting box is assessed by analyzing shear bands formation in the soil. For this purpose, first, some modifications are applied to the direct shear box in the Earthquake Research Institute. In this regard, two blocks are constructed at an angle of 45 degrees that can be moved relative to each other. Transparent walls are utilized to elevate the static resistance, and four screws are installed on the floor of the device. The friction in the test is decreased by using a number of ball bearings. The required thickness for the box walls is determined using a numerical simulation in ABAQUS software. To investigate faulting in granular

soils, Firoozkooh sand is utilized and placed in the developed shear box. Furthermore, the overhead load is first applied by embedding a rubber membrane containing water and applying air pressure to it. By continuous imaging of soil profiles, alterations in the soil surface are recorded, and image correlation method is employed to predict the amount of fault propagation, strain, and dilation. Results affirm that the dilation effect elevates with increasing moisture content and wanes with the addition of fine-grained percentage and by boosting vertical loads. Additionally, different behavior has been observed without softening for cementitious sands.

#### FUNDING/SUPPORT

Not mentioned any Funding/Support by authors.

#### ACKNOWLEDGMENT

Not mentioned by authors.

#### AUTHORS CONTRIBUTION

This work was carried out in collaboration among all authors.

#### CONFLICT OF INTEREST

The author (s) declared no potential conflicts of interests with respect to the authorship and/or publication of this paper.

## 5. REFERENCES

- [1] Papadimitriou EE, Karakostas VG, Papazachos BC. Rupture zones in the area of the 17.08. 99 Izmit (NW Turkey) large earthquake (Mw 7.4) and stress changes caused by its generation. *Journal of Seismology*. 2001 Apr;5(2):269-76. [\[View at Google Scholar\]](#); [\[View at Publisher\]](#).
- [2] Felzer KR, Becker TW, Abercrombie RE, Ekström G, Rice JR. Triggering of the 1999 Mw 7.1 Hector Mine earthquake by aftershocks of the 1992 Mw 7.3 Landers earthquake. *Journal of Geophysical Research: Solid Earth*. 2002 Sep;107(B9):ESE-6. [\[View at Google Scholar\]](#); [\[View at Publisher\]](#).
- [3] Chen YG, Lai KY, Lee YH, Suppe J, Chen WS, Lin YN, Wang Y, Hung JH, Kuo YT. Coseismic fold scarps and their kinematic behavior in the 1999 Chi - Chi earthquake Taiwan. *Journal of Geophysical Research: Solid Earth*. 2007 Mar;112(B3). [\[View at Google Scholar\]](#); [\[View at Publisher\]](#).
- [4] Xiao H, Ivancic R, Zhang G, Riggelman R, Liu A, Durian D. Strain localization and shear band formation during tensile tests of disordered floating granular monolayers. *Bulletin of the American Physical Society*. 2020 Mar 5;65. [\[View at Google Scholar\]](#); [\[View at Publisher\]](#).
- [5] Thomas TY. Plastic flow and fracture in solids. *Journal of Mathematics and Mechanics* 1958:291–322. [\[View at Google Scholar\]](#); [\[View at Publisher\]](#).
- [6] Alshibli KA, Batiste SN, Sture S. Strain localization in sand: plane strain versus triaxial compression. *Journal of Geotechnical and Geoenvironmental Engineering*. 2003 Jun;129(6):483-94. [\[View at Google Scholar\]](#); [\[View at Publisher\]](#).
- [7] Mühlhaus HB, Vardoulakis I. The thickness of shear bands in granular materials. *Geotechnique*. 1987 Sep;37(3):271-83. [\[View at Google Scholar\]](#); [\[View at Publisher\]](#).
- [8] Bray JD, Seed RB, Cluff LS, Seed HB. Earthquake fault rupture propagation through soil. *Journal of Geotechnical Engineering*. 1994 Mar;120(3):543-61. [\[View at Google Scholar\]](#); [\[View at Publisher\]](#).
- [9] Zhu H, Zhou WH, Yin ZY. Deformation mechanism of strain localization in 2D numerical interface tests. *Acta Geotechnica*. 2018 Jun;13(3):557-73. [\[View at Google Scholar\]](#); [\[View at Publisher\]](#).
- [10] Hazeghian M, Soroush A. DEM-aided study of shear band formation in dip-slip faulting through granular soils. *Computers and Geotechnics*. 2016 Jan 1;71:221-36. [\[View at Google Scholar\]](#); [\[View at Publisher\]](#).
- [11] Zhou W, Yang L, Ma G, Xu K, Lai Z, Chang X. DEM modeling of shear bands in crushable and irregularly shaped granular materials. *Granular Matter*. 2017 May;19(2):1-2. [\[View at Google Scholar\]](#); [\[View at Publisher\]](#).
- [12] Kollmer JE, Shreve T, Claussen J, Gerth S, Salamon M, Uhlmann N, Schröter M, Pöschel T. Migrating shear bands in shaken granular matter. *Physical Review Letters*. 2020 Jul 21;125(4):048001. [\[View at Google Scholar\]](#); [\[View at Publisher\]](#).
- [13] Joer H, Lanier J, Desrues J, Flavigny E. "1? 2?": A New Shear Apparatus to Study the Behavior of Granular Materials. *ASTM International*; 1992. [\[View at Google Scholar\]](#); [\[View at Publisher\]](#).
- [14] Lo SC, Chu J, Lee IK. Investigation of the strain-softening behavior of granular soils with a new multiaxial cell. *Geotechnical Testing Journal*. 1994 Sep 1;17(3):325-36. [\[View at Google Scholar\]](#); [\[View at Publisher\]](#).
- [15] Stone KJ, Brown TA. Simulation of ground loss in centrifuge model tests. *Geotechnical Testing Journal*. 1993 Jun 1;16(2):253-8. [\[View at Google Scholar\]](#); [\[View at Publisher\]](#).
- [16] Wang JJ, Zhang HP, Wen HB, Liang Y. Shear strength of an accumulation soil from direct shear test. *Marine Georesources & Geotechnology*. 2015 Mar 4;33(2):183-90. [\[View at Google Scholar\]](#); [\[View at Publisher\]](#).
- [17] Ahmadi M, Moosavi M, Jafari MK. Water content effect on the fault rupture propagation through wet soil-using direct shear tests. In *Advances in Laboratory Testing and Modelling of Soils and Shales* 2017 Jan 18 (pp. 131-138). Springer, Cham. [\[View at Google Scholar\]](#); [\[View at Publisher\]](#).